Growth of Gyroid Grains in the Complex Phase Window of PS-*b*-PI/PS Blends

Vincent H. Mareau,[†] Tadashi Matsushita,[‡] Eiji Nakamura,[§] and Hirokazu Hasegawa*,[†]

Department of Polymer Chemistry, Graduate School of Engineering, Kyoto University, Nishikyo-ku, Kyoto 615-8510, Japan; Kuraray Co. Ltd., 41 Miyukigaoka, Tsukuba, Ibaraki 305-0841, Japan; and Asahikasei Co. Ltd., 2-1 Samejima, Fuji, Shizuoka 416-8501, Japan

Received April 17, 2007; Revised Manuscript Received July 9, 2007

ABSTRACT: The nonequilibrium microphase separation process taking place in polystyrene-*block*-polyisoprene (SI)/polystyrene (hS) blends during solvent evaporation was investigated by transmission electron microscopy to find a way to grow large gyroid single grains free of defects to be used as photonic crystals. Complex microdomain morphologies—gyroid, perforated layers (PL), and sponge—were found in a narrow region of the blend composition (complex phase window), and two different gyroid growth paths were identified for different blend compositions, both of them following a nucleation and growth process but resulting in different gyroid grain qualities. (1) 64/36 wt % (SI/hS): gyroid grains grow from sponge phase and reject part of the hS finally trapped as defects when small grains coagulate to form larger imperfect gyroid grains. (2) 67/33 wt % (SI/hS): gyroid and PL grains nucleate and grow consuming sponge, and then gyroid consumes faster growing PL. The lower nucleation density of gyroid grains results in defect-free large grains though surrounded by a small amount of accumulated hS domains. The second growth path, still requiring improvements, offers a promising method to grow large gyroid single crystals.

Introduction

Diblock copolymers in the strong segregation regime undergo microphase separation to form regular periodic microdomain structures with various morphologies such as spheres, cylinders, bicontinuous networks, and lamellae.[1−8] Since the repeat distances are on the order of the radii of gyration of the copolymers, they vary from less than 10 nm for the smallest extreme to a few hundred nanometers for the high end. Thus, a variety of applications of the microdomain structures are feasible and studied by many researchers. Thomas et al.[9] suggested using the microdomains of high molecular weight diblock copolymers as photonic crystals with which one can manipulate light in many ways. Among the various microdomain morphologies, the gyroid bicontinuous double network structure[10] may be the most fascinating one because a three-dimensional photonic crystal[11] can be prepared with it. From a theoretical point of view, single networks rather than double networks are preferable because complete photonic gaps exist for single networks but not for double networks like the regular gyroid morphology of diblock copolymers as pointed out by Maldovan et al.[12] However, they also suggested that double networks are still useful if the double networks are chemically distinct (to enable selective removal of one network with the matrix phase or to get the refractive index of one network identical to the one of the matrix). From this point of view, it is worth to understand the growth behavior of the gyroid phase as a model system. However, a recent work[13] shows that a photonic band gap can be obtained for ultrahigh-molecular-weight diblock copolymers with various microdomain morphologies including a gyroid double network structure in contrast to the theoretical prediction. To prepare a photonic crystal with gyroid structure, three problems need to be solved: (1) how to control the morphology and the domain size, (2) how to increase the size of gyroid grains, and (3) how to obtain the large enough refractive index difference for the two phases.

Gyroid microdomains, which were first misinterpreted as OBDD network structure,[5,14,15] are observed for the diblock copolymers with a narrow range of composition between cylinders and lamellae.[5,6] This compositional region is known as "complex phase window"[16,17] since complex morphology such as hexagonally perforated layers (HPL) in addition to gyroid appear in this region. Synthesis of a diblock copolymer having gyroid microdomains with a few hundred nanometers domain spacing is however extremely difficult, as extremely high molecular weight ($>10^6$ g/mol) and a precise composition are required.

Blending homopolymers to diblock copolymers is a well-known technique to control microdomain morphology and domain sizes.[18−25] It was reported that the bicontinuous network morphology, which must have been gyroid but were interpreted as OBDD judged by the "wagon-wheel" pattern in the 2D TEM images, could be obtained by blending polystyrene (hS)[20−23] or poly(vinyl methyl ether)[26,27] with the lamella-forming polystyrene-*block*-polyisoprene (SI) diblock copolymer. In this case, the ratio (r) of the molecular weight of homopolymer (M_h) to that of the corresponding (or miscible) block (M_b) is the key parameter ($r = M_h/M_b$) for the state of mixing between the homopolymer and the block copolymer and, therefore, the resulting microdomain morphology.[18,21,28] When $r \ll 1$, the added homopolymer swells the corresponding block chains (wet brush regime) to change the interfacial mean curvature, which may result in a morphological transition as well as some increase in domain size.[18,21] On the other hand, when $r \sim 1$, the added homopolymer is mixed into the corresponding microdomains without swelling the block chains and localized in the middle regions of the microdomains (dry brush regime).[28] Thus, interfacial mean curvature and microdomain morphology do not change while domain size is greatly expanded if the homopoly-

* To whom correspondence should be addressed. E-mail: hasegawa@alloy.polym.kyoto-u.ac.jp.
[†] Kyoto University.
[‡] Kuraray Co. Ltd.
[§] Asahikasei Co. Ltd.

10.1021/ma0708996 CCC: $37.00
Published on Web 08/18/2007

mer of the major component with $r \sim 1$ is added. If we employ the homopolymer in the wet brush regime but very close to the limit, we should be able to control the interfacial mean curvature for gyroid morphology and maximize the domain size at the same time.

So far, diblock copolymer/homopolymer blends have been mainly studied in the thermal equilibrium regime, and the phase diagrams were obtained for relatively low-molecular-weight polymers. Thermal equilibrium states of block copolymer/homopolymer blends of relatively high molecular weights are difficult to attain by annealing due to the high viscosity. Therefore, morphology of relatively high-molecular-weight block copolymers has been studied mainly for as-cast films. However, the observed morphology in as-cast films depends on the casting conditions such as casting solvents, temperature, evaporation rate of solvent, etc. Nevertheless, no systematic work to investigate the self-assembling process of block copolymer/homopolymer blends during solution casting has been reported yet.

In this study, we investigated, as a function of the solution casting process, the evolution of the microdomain morphology of SI diblock copolymer/hS homopolymer blends with relatively high molecular weight in the wet brush regime but near the limit to the dry brush regime. Our final goal is to establish a technique to prepare a giant single grain of gyroid microdomains with a large enough domain size for photonic crystal applications. However, as a first attempt we used somewhat smaller molecular weight polymers for convenient transmission electron microscope (TEM) observations. By finely tuning the blend composition, we located the complex phase window in the blends with very narrow composition range where gyroid, perforated layer (PL), sponge, and so on were observed. Since the structures in the as-cast films are nonequilibrium structures, the coexistence of several different microdomain structures was observed in addition to localized macrophase separation. By tuning solvent evaporation rate, we could observe the evolution of the microdomains structures in the as-cast films, from which the self-assembling process in the solution was conjectured.

In the complex phase window, self-assembly of the blend in solution starts first with the growth of an irregular network structure (sponge) followed by regular structures (gyroid and PL), nucleating and growing from sponge. Gyroid seems to be the stable structure since gyroid grains appear to grow consuming both sponge and PL. During the course of this study we found large "gyroid single crystals", large monograins of gyroid surrounded by other morphologies. This technique may be a possible route to grow large single crystal-like gyroid grains to be used as photonic crystals.

Experimental Section

Materials. A polystyrene-*block*-polyisoprene (SI) diblock copolymer and a polystyrene homopolymer (hS) were synthesized via living anionic polymerization with *sec*-butyllithium as an initiator and cyclohexane as a solvent. The molecular weight, $M_n = 7.9 \times 10^4$ (SI) and $M_n = 4.4 \times 10^4$ (hS), and composition of the copolymer, 62 wt % (58 vol %) of S, were measured by gel permeation chromatography (GPC) and ^{1}H NMR spectroscopy, respectively. This gives $r = 0.90$ (wet brush regime, close to dry brush[1]). Polydispersity indices of 1.16 (SI) and 1.03 (hS) were measured by GPC. Blends with compositions ranging from 60/40 to 80/20 w/w (SI/hS) were prepared by dissolving both polymers in toluene at 10% w/v. (Toluene is a neutral solvent for both PS and PI and was chosen for this reason.) This corresponds to blends with a PS (S + hS) volume fraction ranging from 74% to 66%, respectively.

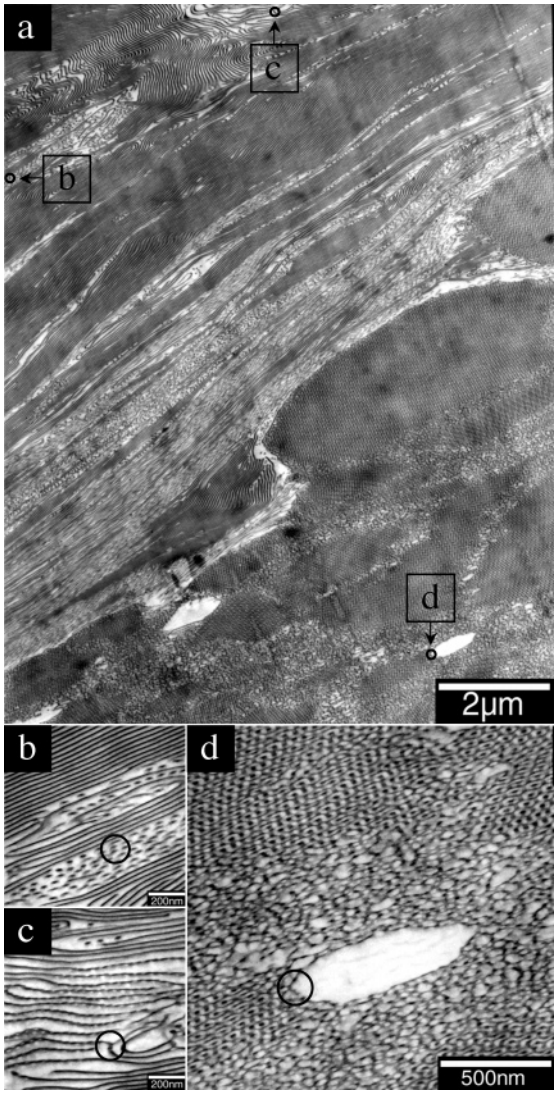

Figure 1. TEM images of the 64/36 SI/hS blend, slow evaporation (2 weeks). Reference circles (diameter 150 nm) in the main TEM image (a) enable localization of the enlarged areas (b−d). Coexisting morphologies of microphase-separated domains are observed: (b) lamellae, and cylinders; (c) lamellae, cylinders and PL; (d) gyroid, sponge, and hS.

Sample Preparation. Films were prepared by casting polymer solutions, followed by subsequent solvent evaporation over different length of time, 1−2 min (in a vacuum oven), 24 h, 5 days, and 2 and 4 weeks, from very fast to very slow evaporation rates. Films obtained were further dried under vacuum for 2 days at room temperature (no annealing). Ultrathin sections (50 nm) were cut on a Reichert Ultracut E ultramicrotome at −100 °C using a cryo kit (Leica EM FCS). Sections were stained with the vapors of 2 wt % O_sO_4(aq) at room temperature for 1 h (selective staining of the polyisoprene phase, darker in TEM images).

Transmission Electron Microscopy (TEM). The microdomain structures were observed under a transmission electron microscope (TEM, JEOL JEM-2000FXZ) operated at 200 kV.

Results and Discussion

The multiphasic morphology characteristic of the blend studied is presented in Figure 1. For this blend composition, 64/36 (SI/hS), we can observe coexisting morphologies such as lamellae, cylinders, gyroid, sponge,[29,30] perforated layers (PL), and hS domains. It should be stressed that identification of the bicontinuous morphology as gyroid was not performed by SAXS (domain spacing too large) but by 3D TEM (results not

Table 1. Morphologies of Microphase-Separated Domains, Obtained after a Slow Evaporation (2 weeks) as a Function of the SI/hS Blend Composition

SI (wt %)	63−66	67	68−76
morphologies	lamellae cylinders	lamellae gyroid	lamellae perforated layers
	gyroid	perforated layers	
	sponge perforated layers		
PS(S + hS) (vol %)	73−72	71	71−68

presented here but submitted for publication). In Figure 1a we observe mainly lamellae and few PL and cylinders in the upper left corner (location of Figure 1b,c), gyroid grains and localized hS domains in a sponge matrix in the lower right corner (location of Figure 1d), and mainly cylinders with few lamellae for the rest (diagonal from upper right to lower left). This sample was obtained after a slow evaporation of the solvent, over a period of 2 weeks, and exhibits clear concentration fluctuations of hS resulting from the self-assembly process. Indeed, some areas of the TEM images appear brighter than others; this results from higher hS content, up to pure hS domains. In these conditions, the cast film does not have a thermodynamically equilibrated structure, but instead the different microdomain structures may be reflecting equilibrium morphologies for the local composition of the blend. The origin of the nonequilibrium behavior of this system comes from the use of a solvent evaporation process, not followed by any annealing, the high molecular weight of the polymers, and the respective dimensions of S block and hS homopolymer ($r = 0.90$: wet brush regime, but close to dry brush). Such nonequilibrium structures were not previously studied in detail as reproducible results are difficult to obtain. However, this problem can be overcome by monitoring the evaporation rate of solvent, and thus the film-casting processes can be defined.

The detailed observation of TEM images of this complex system can provide important information with regard to order−order transitions and growth mechanism of particular microdomain morphology, formation, and annihilation of various kinds of defects, including grain boundaries, etc. To this purpose, we can compare morphologies observed for different evaporation times, as well as in a single sample, and morphologies observed at different locations, corresponding to different stages of the same transition process. The blend composition presented in Figure 1 is especially interesting because it exhibits plural complex bicontinuous morphologies like gyroid, sponge, and PL. To determine the composition range for which these morphologies are observed, we analyzed by TEM the composition dependence of the microdomain morphology by 1% increment from 60 to 80 wt % of SI for as-cast films prepared by slowly removing the solvent over a period of 2 weeks at room temperature. The results are presented in Table 1. For blends with less than 63 wt % SI, only cylindrical microdomains and lamellar vesicles were observed, in addition to macroscopic hS domains. For blends with more than 76 wt % SI, only lamellar microdomains were observed, which correspond to the morphology of neat SI. For blends with SI weight percent between 63 and 76%, complex structures such as sponge, gyroid, and PL are observed, giving this composition range its name "complex phase window".

Within this complex phase window, with increasing hS amount, the PL morphology appears first, followed by gyroid and sponge. In addition, for the composition range where gyroid is observed (63−67 wt % SI), we found two different situations: (1) gyroid grains are surrounded by sponge (64−66 wt % SI) as observed in Figure 1; (2) gyroid grains are surrounded by PL (67 wt % SI). In order to better understand the development of the gyroid phase, we focused on these two different cases and studied in more detail the 64 and 67 wt % SI blends, which are representative of each situation. N.B.: the total volume percent of PS (S + hS) is indicated in Table 1 as a reference, and it should not be forgotten that the blend composition is not homogeneous, which explains why the gyroid morphology is observed here between 71 and 73 vol % PS whereas this morphology is usually observed for 64−67 vol % PS[22] for homogeneous systems.

Development of the Gyroid Phase for the 64/36 Blend Composition. For this composition, 64/36 (SI/hS), after evaporation of the solvent over a period of 2 weeks, the gyroid grains are embedded in a sponge matrix. This phenomenon has already been described in Figure 1 and is illustrated by Figure 2a−c, with TEM images taken from a unique sample, but showing gyroid grains presumably observed at different steps of a single growth process. From a large set of observations we can assume that the gyroid develops through a nucleation and growth process, as already observed in solution.[31] Figure 2a corresponds to the nucleation of the gyroid phase inside of the sponge phase, Figure 2b, at a later stage, shows the collision and coagulation of gyroid grains, and finally Figure 2c displays the development of gyroid grain facets and the expulsion of excess hS leading to the formation of pure hS domains. Indeed, 64 wt % SI corresponds to 73 vol % PS, at least 6 points above the maximum observed limit for gyroid growth (67 vol % PS); therefore, part of the hS cannot be consumed by the growing gyroid. The leftover hS is first localized in the sponge phase and finally develops as pure hS domains in the center of the trapped sponge phase.

To observe the development of larger gyroid grains, we used the same blend composition but chose a lower evaporation rate: over 4 weeks instead of 2. We indeed obtained larger gyroid grains but also found many trapped defects, like sponge and hS domains, and a large amount of hS accumulated around the gyroid grain, as illustrated by Figure 2d−h. In Figure 2d, the large gyroid grain (several tens of micrometers) is surrounded by lamellae and rejected hS. Detailed analysis of this sample is provided by Figure 2e−h, with TEM images obtained for bigger enlargements. Figure 2e shows the presence of lamellar vesicles[28] in the hS-enriched area of the lamellar phase surrounding the gyroid grain. We can see that the lamellar phase can accommodate a large amount of hS by swelling and deformation. Both the gyroid and Lamellar phase have to expel hS to grow, which explains the large amount of hS found at this gyroid−lamellae grain boundary, compare to gyroid−sponge grain boundaries. Figure 2f shows the perfection of the gyroid phase observed in the grain, away from the sponge and hS defects. Parts g and h of Figure 2 present two types of defects, i.e., trapped hS phase in direct contact with gyroid or separated by a layer of sponge phase, respectively. As the dimension of the defect of Figure 2g is much smaller than the one of Figure 2h, one can expect that in the case of Figure 2g all the sponge phase has been consumed by the gyroid phase, leaving only the hS leftover, whereas in Figure 2h, some sponge phase remains to be consumed by the gyroid phase and would have been if the process would not have been stopped by the solvent evaporation.[32] The presence of a defect with an intermediate state (small layer of sponge) at the bottom right corner of Figure 2d supports this conclusion.

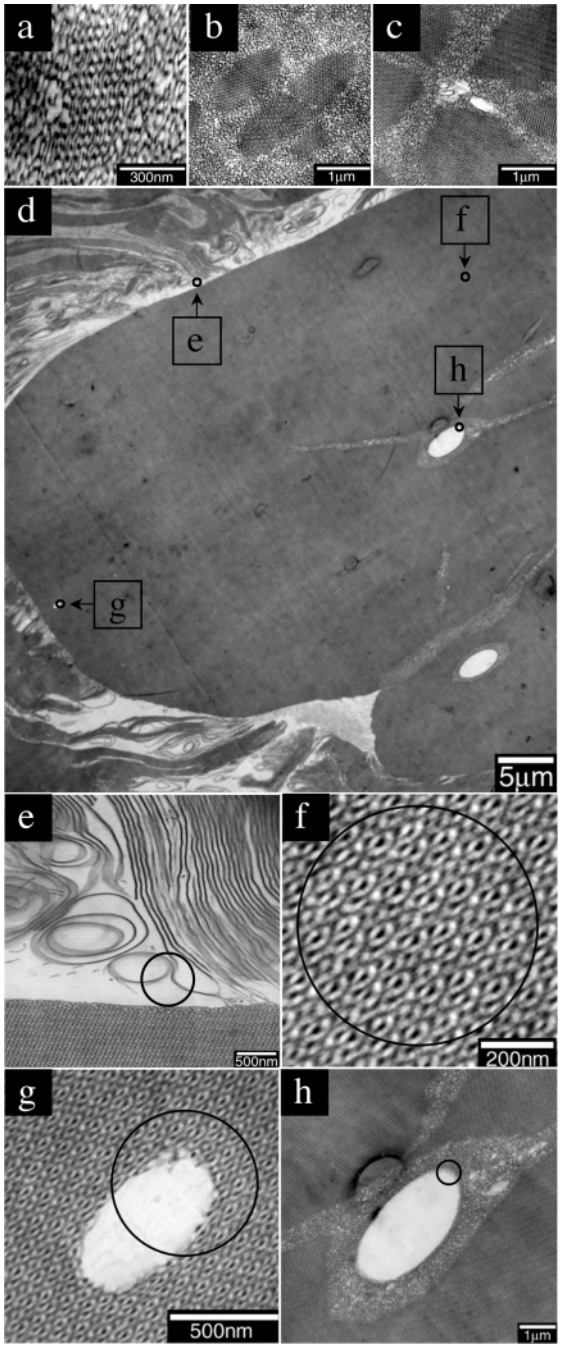

Figure 2. TEM images of the 64/36 SI/hS blend, after a slow evaporation of 2 weeks (a−c) and 4 weeks (d−h). Reference circles (diameter 700 nm) in TEM image (d) enable localization of the enlarged areas (e−h). Large gyroid grains are observed with accumulated hS and sponge trapped defects.

A schematic drawing, presented in Figure 3, illustrates the proposed mechanism for the development of the gyroid phase from the sponge phase in the 64/36 blend composition. First, in Figure 3a, only sponge is present, which was conjectured since only sponge phase is observed in the blend films when the solvent is quickly removed by pumping in a vacuum oven. Then gyroid nuclei appear in Figure 3b, as shown for the case of 67/33 blend below, and grow with their respective lattice orientation consuming the sponge phase. Part of the hS from the sponge phase is excluded from the gyroid phase and starts to form a pure hS phase in Figure 3c. In Figure 3d, the gyroid grains start to merge; the pure hS phase forms now a defect in the center of the gyroid domain and gets bigger as the sponge phase is being consumed. A pure hS layer is also observed

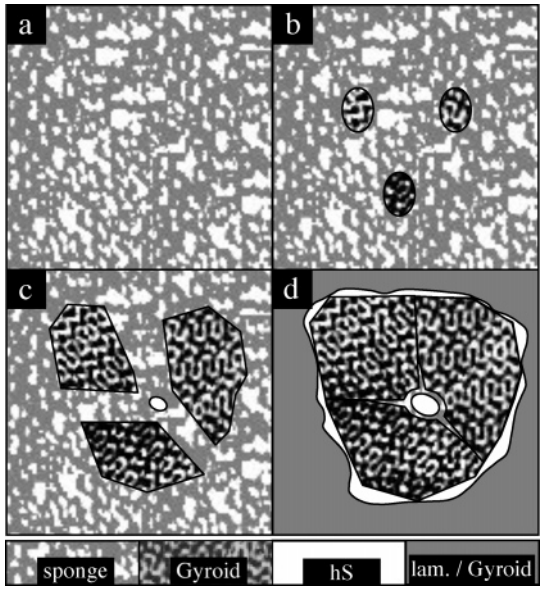

Figure 3. Schematic drawing illustrating the growth path of the gyroid phase for the 64/36 blend composition: growth from the sponge phase resulting in gyroid grains with defects (trapped hS and sponge phase).

surrounding the gyroid domain, after consumption of the sponge phase by the gyroid and the surrounding morphologies (other gyroid grains or lamellae). One phenomenon not described in this scheme is the reorganization that takes place inside of the gyroid domain to go from polygrain to single grain morphology. Indeed, in Figure 2d only one gyroid lattice orientation is observed in the large gyroid grain, and this is a general observation for the blend studied. It is indeed nearly impossible to find a gyroid/gyroid grain boundary in this sample. Therefore, we assume that the gyroid networks can easily modify their lattice orientation due to their cubic symmetry and achieve a uniform orientation when merging. However, we did not observe the different steps of this process.

Development of the Gyroid Phase for the 67/33 Blend Composition. For the composition, 67/33 (SI/hS), after a slow evaporation over a period of 2 weeks, the gyroid grains are embedded in a PL matrix. To understand the growth path of the gyroid phase for this blend composition, we used a combination of evaporation times to stop the growth at different stages. In this way, Figure 4a−d presents TEM images obtained after full solvent evaporation in 1−2 min (by pumping in a vacuum oven) (a), 24 h (b, c), and 5 days (d) to reveal the ordering process. In Figure 4a, only sponge phase is observed after very fast solvent evaporation. When longer time is offered for ordering, with solvent evaporated in 24 h, PL and gyroid nuclei are found, as presented in parts b and c of Figure 4, respectively. Figure 4b shows some resemblance in the morphology reported by Laurer et al.,[33] who observed the coexistence of swollen lamellae and sponge phases in a SI diblock copolymer/hS homopolymer blend. It should be noticed that the PL nuclei have an ellipsoidal shape with the layer normal parallel to the long axis of the ellipsoids to minimize the interfacial energy. Indeed, interfacial tension at the grain boundary depends on the orientation of the PL layers with respect to the grain boundary, and our observations show that interfacial tension decreases when PL layers are perpendicular to the boundary, i.e., the continuous microdomain interfaces for each component at the grain boundary. This is in agreement with the observation of lamellar nuclei reported by Sakamoto and Hashimoto[34] in the SI diblock copolymer melt and with the theoretical predictions by Hohenberg and Swift.[35] For a

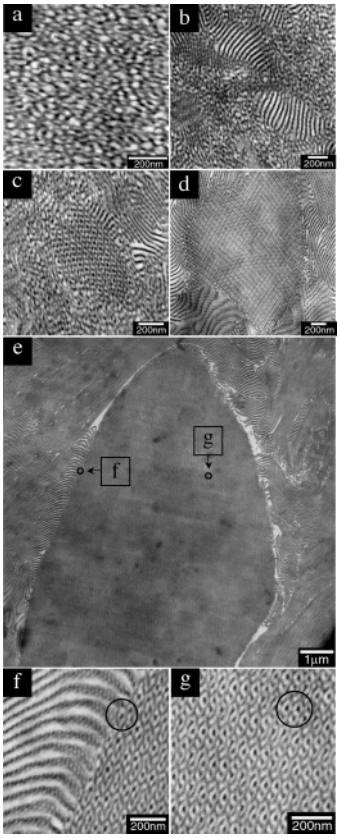

Figure 4. TEM images of the 67/33 SI/hS blend, after different evaporation times: fast (1−2 min) (a); 24 h (b, c); 5 days (d); 2 weeks (e−g). Reference circles (diameter 150 nm) in TEM image (e) enable localization of the enlarged areas (f, g). Sponge phase is observed alone after fast evaporation, PL and gyroid nuclei are observed in the sponge phase for 24 h evaporations, and only gyroid and PL are observed for 5 days and 2 weeks evaporations. Large gyroid grains are observed without trapped defects.

longer evaporation time of 5 days, only gyroid and PL phases are found; all the sponge has been consumed, as illustrated by Figure 4d. We found that PL phase develops faster than gyroid (larger grains observed), and at an early stage, the gyroid has to consume PL instead of sponge. The resulting shape of the gyroid grains is then more irregular, without facets, compared to what is observed for the 64/36 blend composition. Indeed, contrary to the sponge phase, the PL phase is anisotropic, and the growth rate of gyroid grains depends on the relative orientation of the PL grains at the gyroid/PL grain boundary: a faster growth rate is observed when PL layers are perpendicular to the grain boundary. (This conclusion is drawn from a large number of observations and not from the few images presented in Figure 4.) Indeed, perpendicular orientation of the PL layers relative to the grain boundary enables the connection of the PS and PI microdomains of the gyroid and PL grains through the grain boundary, which is not true for parallel orientation. We assume that polymer chains can diffuse faster when microdomains are continuous, which explains the faster growth rate observed for the gyroid. Another difference observed for this blend compared to the 64/36 composition is the much lower gyroid nucleation density which allows for larger gyroid grains to grow undisturbed, before merging onto each other. This lower gyroid nucleation density results from the competition between gyroid and PL nuclei in the 67/33 blend. As the gyroid nucleation is sporadic (grains of very different dimensions are observed, indicating different nucleation time) and the PL growth rate is much faster than that of gyroid, the sponge

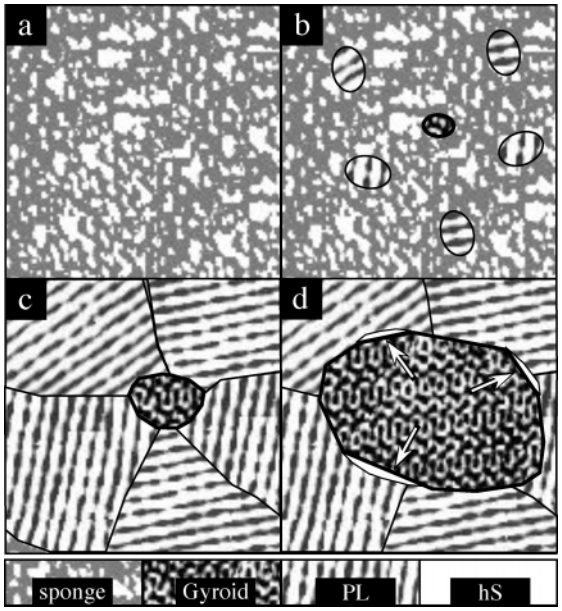

Figure 5. Schematic drawing illustrating the growth path of the gyroid phase for the 67/33 blend composition: lower nucleation density and growth from the PL phase resulting in large gyroid grains without trapped defects.

volume where gyroid can nucleate decreases fast and so does the nucleation density of gyroid grains.

In this way, Figure 4e illustrates the large growth achieved by a gyroid grain in a sample evaporated over a period of 2 weeks. A gyroid grain about 10−20 μm is observed, surrounded by PL grains and small amount of hS leftover. No large defect, like sponge phase or hS trapped, is observed in the gyroid grain, and small lattice defects if they exist are not clear and difficult to identify. Parts f and g of Figure 4 are TEM images of the same sample obtained for bigger enlargements, displaying details of the gyroid/PL grain boundary and of the high regularity of the gyroid lattice, respectively. As observed in Figure 4e,f, layers of the PL phase often appear bent at the vicinity of the gyroid grain, like if they would adjust locally their orientation to be perpendicular to the grain boundary. Indeed, the energetic cost of the ruptures of the PS and PI microdomains is minimized for the perpendicular orientation. Contrarily, a larger number of ruptures are necessary when PL layers are parallel to the grain boundary. The smaller amount of pure hS domains surrounding the gyroid grains compared to the previous composition studied is related to the lower amount of hS found in this blend (33 vs 36 wt %). Still, there is certainly too much hS left over to grow very large gyroid single crystals at this blend composition, as it would finally form a barrier layer preventing further growth of the gyroid grain.

A schematic drawing is presented in Figure 5 to illustrate the proposed mechanism for the development of the gyroid phase from the sponge and then PL phases in the 67/33 blend composition. First, in Figure 5a, only sponge is present, and then PL and gyroid nuclei appear in Figure 5b and develop with their respective growth rates, consuming the sponge phase. In Figure 5c, the gyroid grain is surrounded by PL grains and thus grows, consuming the PL phase instead of sponge. Finally in Figure 5d, after some growth, pure hS phase is observed on some location at the gyroid/PL grain boundary, and a large gyroid grain free of trapped defect is obtained.

Conclusions. In this work we investigated the nonequilibrium multiphase structures obtained in solution cast films of SI/hS blends by TEM. Comparing the morphology of the same blend

samples prepared by different solvent evaporation conditions enabled us to conjecture the ordering process during solvent evaporation. We found the existence of a narrow region in the blend composition where complex microdomain morphologies such as gyroid, PL, and sponge are observed (complex phase window).

In this composition range, sponge microdomains seem to grow from the disordered mixture as the concentration of the solution increases. We found that the gyroid phase, one of the stable structures in the complex window, can consume the sponge phase by a nucleation and growth process. Depending on the blend composition, it was found that the gyroid grains grow solely from the sponge phase (64 wt % SI) or successively from the sponge and the PL phases (67 wt % SI). In both cases, rearrangements of the network structures from one morphology to the other induce small adjustments of the blend composition; i.e., excess hS is expelled from gyroid microdomains. As 67/33 blend contains less hS than 64/36 blend, the amount of hS accumulated in pure hS domains at the periphery of gyroid domains is logically lower in the 67/33 blend. In addition, as PL grains grow much faster than gyroid ones, the nucleation density of gyroid is lower in the 67/33 blend than in the 64/36, and therefore collision and coagulation of gyroid grains seldom occur in the 67/33 blend, resulting in "single-crystal"-like gyroid grains with no large defects. Oppositely, large gyroid grains observed in the 64/36 blend always result from the coagulation of smaller grains and present defects like hS and sponge inclusions introduced by this process. In a remarkable way, however, it was observed that gyroid networks of the initial independent grains rearrange to form a single grain, which is a very important result in the quest of very large gyroid grains for photonic crystal applications.

Thus, in the SI/hS blends complex phase window, we found two mechanisms for the growth process of gyroid microdomains during films casting from solution, and one of them could be useful to grow large gyroid grains without defects. The blend strategy instead of pure copolymers offers access to higher domains spacing (mandatory for photonic applications), without issues related to the synthesis of high-molecular-weight copolymers, and to difficult microphase separation in such high-viscosity systems. However, as reported here, the problematic accumulation of pure hS at the periphery of the gyroid grains has to be solved to obtain larger gyroid single crystals. Our results show that adjustments of the composition of the blend alone cannot solve the problem as no gyroid is observed for the 68/32 blend composition, just 1% away from the 67/33 blend presented here. Therefore, a solution could be the application of an external force to the system during microphase separation to enhance the mobility of the hS phase accumulated at the periphery of the gyroid grains and therefore to break this barrier. This would offer to the gyroid grain a permanent access to consumable PL phase and supposedly a continuous growth. Samples used in this study were evaporated in a quiescent state, away from vibrations, and we are now investigating slow evaporation conditions involving moderate vibrations of the solution to obtain very large gyroid photonic crystals.

Acknowledgment. This work was supported in part by a Grant-in-Aid for Scientific Research (under Grant 17105004-(S)) from the Japan Society for the Promotion of Science. V.H.M. thanks JSPS (Postdoctoral Research Program P05746) for generous financial support.

Supporting Information Available: A graph presenting the evolution of polymer concentration with casting time for 2 and 4 weeks cast and TEM images illustrating localized accumulations of hS prohibiting the growth of gyroid microdomains for 67/33 blend composition. This material is available free of charge via the Internet at http://pubs.acs.org.

References and Notes

(1) Hamley, I. W. *The Physics of Block Copolymers*; Oxford University Press: Oxford, 1998.
(2) Molau, G. E. In *Block Copolymers;* Aggarwal, S. L., Ed.; Plenum: New York, 1970.
(3) Meier, D. J. In *Block and Graft Copolymers*; Burke, J. J., Weiss, V., Eds.; Syracuse University Press: New York, 1973.
(4) Leibler, L. *Macromolecules* **1980**, *13*, 1602−1617.
(5) Hasegawa, H.; Tanaka, H.; Yamasaki, K.; Hashimoto, T. *Macromolecules* **1987**, *20*, 1651−1662.
(6) Khandpur, A. K.; Förster, S.; Bates, F. S.; Hamley, I. W.; Ryan, A. J.; Bras, W.; Almdal, K.; Mortensen, K. *Macromolecules* **1995**, *28*, 8796−8806.
(7) Matsen, M. W.; Schick, M. *Phys. Rev. Lett.* **1994**, *72*, 2660−2663.
(8) Matsen, M. W.; Bates, F. S. *Macromolecules* **1996**, *29*, 1091−1098.
(9) Edrington, A. C.; Urbas, A. M.; DeRege, P.; Chen, C. X.; Swager, T. M.; Hadjichristidis, N.; Xenidou, M.; Fetters, L. J.; Joannopoulos, J. D.; Fink, Y.; Thomas, E. L. *Adv. Mater.* **2001**, *13*, 421−425.
(10) Hajduk, D. A.; Harper, P. E.; Gruner, S. M.; Honeker, C. C.; Kim, G.; Thomas, E. L.; Fetters, L. J. *Macromolecules* **1994**, *27*, 4063−4075.
(11) Martin-Moreno, L.; Garcia-Vidal, F. J.; Somoza, A. M. *Phys. Rev. Lett.* **1999**, *83*, 73−75.
(12) Maldovan, M.; Urbas, A. M.; Yufa, N.; Carter, W. C.; Thomas, E. L. *Phys. Rev. B* **2002**, *65*, 165123-1−165123-5.
(13) Tominaga, J.; Mori, N.; Hara, S.; Yamamoto, K.; Okamoto, S.; Hasegawa, H.; Kobayashi, T.; Koshikawa, N.; Sano, S. *Polym. Prepr. Jpn.* **2007**, *56*, 744.
(14) Thomas, E. L.; Alward, D. B.; Kinning, D. J.; Martin, D. C.; Handlin, D. L., Jr.; Fetters, L. J. *Macromolecules* **1986**, *19*, 2197−2202.
(15) Hajduk, D. A.; Harper, P. E.; Gruner, S. M.; Honeker, C. C.; Thomas, E. L.; Fetters, L. J. *Macromolecules* **1995**, *28*, 2570−2573.
(16) Hanley, K. J.; Lodge, T. P. *J. Polym. Sci., Part B: Polym. Phys.* **1998**, *36*, 3101−3113.
(17) Matsen, M. W.; Bates, F. S. *Macromolecules* **1996**, *29*, 7641−7644.
(18) Hashimoto, T.; Hasegawa, H.; Tanaka, H. *Macromolecules* **1990**, *23*, 4378−4386.
(19) Tanaka, H.; Hasegawa, H.; Hashimoto, T. *Macromolecules* **1991**, *24*, 240−251.
(20) Winey, K. I.; Thomas, E. L.; Fetters, L. J. *J. Chem. Phys.* **1991**, *95*, 9367−9375.
(21) Winey, K. I.; Thomas, E. L.; Fetters, L. J. *Macromolecules* **1992**, *25*, 2645−2650.
(22) Winey, K. I.; Thomas, E. L.; Fetters, L. J. *Macromolecules* **1992**, *25*, 422−428.
(23) Spontak, R. J.; Smith, S. D.; Ashraf, A. *Macromolecules* **1993**, *26*, 956−962.
(24) Matsen, M. W. *Macromolecules* **1995**, *28*, 5765−5773.
(25) Likhtman, A. E.; Semenov, A. N. *Macromolecules* **1997**, *30*, 7273−7278.
(26) Xie, R.; Yang, B.; Jiang, B. *Macromolecules* **1993**, *26*, 7097−7099.
(27) Hasegawa, H.; Hashimoto, T.; Hyde, S. T. *Polymer* **1996**, *37*, 3825−3833.
(28) Koizumi, S.; Hasegawa, H.; Hashimoto, T. *Makromol. Chem., Macromol. Symp.* **1992**, *62*, 75−91.
(29) Hashimoto, H.; Kimishima, K.; Hasegawa, H. *Macromolecules* **1991**, *24*, 5704−5712.
(30) Jinnai, H.; Hasegawa, H.; Nishikawa, Y.; Sevink, G. J. A.; Braunfeld, M. B.; Agard D. A.; Spontak, R. J. *Macromol. Rapid Commun.* **2006**, *27*, 1424−1429.
(31) Chastek, T. Q.; Lodge, T. P. *Macromolecules* **2003**, *36*, 7672−7680.
(32) Mori, K.; Hasegawa, H.; Hashimoto, T. *Polymer* **1990**, *31*, 2368−2376.
(33) Laurer, J. H.; Smith, S. D.; Samseth, J.; Mortensen, K.; Spontak, R. J. *Macromolecules* **1998**, *31*, 4975−4985.
(34) Sakamoto, N.; Hashimoto, T. *Macromolecules* **1998**, *31*, 3815−3823.
(35) Hohenberg, P. C.; Swift, J. B. *Phys. Rev. E* **1995**, *52*, 1828−1845.

MA0708996